SPECIAL REPORT 94-10

Effect of Matrix Stiffness on Wavy Fiber Behavior in Single-Carbon-Fiber-Epoxy Composites

Madhu S. Madhukar and Piyush K. Dutta

April 1994

Abstract

This research identifies the mechanisms responsible for lowering the tensile strength of unidirectional polymer matrix composites at low temperatures. Since the stiffness of polymer matrices increases and toughness decreases when the temperature is lowered, the effect of low temperature was simulated by changing the matrix stiffness and toughness. Composite specimens containing a single carbon fiber embedded in an epoxy matrix were cast. The fibers were cast in curved geometries, and the specimens were loaded in tension. The fiber and interfacial failure processes were observed under polarized and unpolarized light through an optical microscope. Increasing the tensile load on the single fiber–epoxy specimens broke the embedded fiber into small fragments, whose lengths were smaller in the regions where the fiber was lying parallel to the loading axis. A significant fiber/matrix interfacial debonding, observed near the broken fiber ends in all specimens, was much more pronounced when the fiber was at an angle to the loading axis. Transverse tensile stresses at the interface caused this interfacial debonding. Specimens with higher matrix stiffness had long matrix cracks at the broken fiber ends, which were perpendicular to the fiber axis. These matrix cracks tend to propagate perpendicular to the fiber axis, increasing the composite's cold sensitivity. The major conclusions are as follows: 1) When fibers are wavy, they are not loaded to their full capacity because of premature interfacial debonding started by the interfacial shear stresses and the transverse tensile stresses. The transverse tensile stresses at the interface are not present in the straight fiber specimens. 2) At higher stiffness and lower toughness values, the matrix cracks emanating at the broken fiber ends make the composite weaker. These two sources lower the strength of unidirectional composites at low temperatures.

For conversion of SI metric units to U.S./British customary units of measurement consult ASTM Standard E380-89a, *Standard Practice for Use of the International System of Units,* published by the American Society for Testing and Materials, 1916 Race St., Philadelphia, Pa. 19103.

Special Report 94-10

U.S. Army Corps of Engineers
Cold Regions Research & Engineering Laboratory

Effect of Matrix Stiffness on Wavy Fiber Behavior in Single-Carbon-Fiber–Epoxy Composites

Madhu S. Madhukar and Piyush K. Dutta

April 1994

Prepared for
OFFICE OF THE CHIEF OF ENGINEERS

PREFACE

This report was prepared by Dr. Madhu S. Madhukar, Assistant Professor, Engineering Sciences and Mechanics Department, University of Tennessee, Knoxville, and Dr. Piyush K. Dutta, Materials Research Engineer, Applied Research Branch, Experimental Engineering Division, U.S. Army Cold Regions Research and Engineering Laboratory. Funding was provided by the Office of the Chief of Engineers through DA Project 4A762784AT42, *Cold Regions Engineering Technology*; Task SS; Work Unit 019, *Behavior of Materials at Low Temperatures*.

Technical review for this report was provided by Dr. David Hui, University of New Orleans, and Edel Cortez, CRREL.

Effect of Matrix Stiffness on Wavy Fiber Behavior in Single-Carbon-Fiber–Epoxy Composites

MADHU S. MADHUKAR AND PIYUSH K. DUTTA

INTRODUCTION

Experiments on tensile loading of unidirectional composite laminates at low temperatures have shown that the longitudinal tensile strength of these composites drops at these temperatures (Dutta 1992). This research program was undertaken to identify the mechanisms that are responsible for this tensile strength degradation at low temperatures.

It is generally believed that, in unidirectional composites with a high fiber volume fraction, tensile behavior is primarily governed by the fiber properties. The influence of the matrix or the fiber/matrix interface, or both, is not considered to be too significant. These assumptions are based on rule-of-mixture types of relationships and they hold good for tensile modulus. However, for tensile strength and tensile failure modes, the matrix and interface properties also play a significant role (Bader 1988, Madhukar and Drzal 1991). Unlike the compressive failure of uniaxial composites, which happens suddenly and which is driven by the instability of compressively loaded fibers, the longitudinal tensile failure of carbon–epoxy composites is a gradual process, i.e., the load carrying fibers start failing at well below the composite's tensile failure load. After the beginning of fiber failure, the additional tensile load that can be applied to the composite will depend upon how the high local stresses at the broken fiber ends are transferred to the neighboring fibers. The properties of the matrix and interface govern this stress transfer mechanism and thus the tensile strength of composites.

Another factor that may affect the longitudinal tensile strength of composites is fiber waviness that may have been introduced during manufacture. The wavy fiber will be nonuniformly loaded when the composite is subjected to a tensile load. In addition, the interface will also be subjected to shear as well as transverse tensile stresses near the wavy fibers. The interface is likely to fail prematurely under these combined stresses. These problems are expected to be more severe at low temperature, when the matrix has low fracture toughness.

These two issues, i.e., the effects of matrix stiffness and toughness and the wavy fiber geometry on the fiber and interface failure process in single fiber composites, were investigated to understand the mechanisms that cause the strength degradation at low temperatures.

MATERIAL

The fiber used in this study was a high strength, PAN-based AS4 graphite fiber. The matrix material was epoxy, which is a diglycidyl ether of bisphenol-A (EPON 828, Shell Chemical Company) cured with meta-pheylene diamine (m-PDA, Aldrich Chemical Company). Specimens were made with two different ratios of the m-PDA curing agent, namely 14.5 parts per hundred (phr) and 10.0 phr by weight. The epoxy was mixed, debulked in a vacuum at 75°C (167°F) for about 10 minutes and then subjected to a two-step cure cycle in air. In the first cycle, the temperature of the material was increased from room temperature to 75°C (167°F) and held constant for 2 hours. Afterwards, the temperature was increased again to a 125°C (257°F) and held constant for 2 hours. After the second dwell time, the heating cycle was stopped and the specimen was allowed to cool to room temperature. The purpose of the first dwell is to allow gases and other volatiles to escape the matrix material and to allow the matrix to flow. The purpose of the second dwell time is to allow cross-linking of the polymer to take place. The temperature–time curing cycle was applied by means of a quartz strip heater, whose temperature

Table 1. Effect of the m-PDA curing agent ratio on the properties of matrix material.

	E		σ_f		ε_f
	(GPa)	*(Kips/in.²)*	*(MPa)*	*(Kips/in.²)*	*(%)*
EPON 828 cured with 14.5% m-PDA	4.4	634	50	7.2	2.30
EPON 828 cured with 10% m-PDA	4.7	688	44	6.4	1.27

was controlled by a thermostat and a power distributor. The temperature–time histories were recorded on a Macintosh IIci computer.

EXPERIMENTAL PROCEDURE

In the case of EPON 828 matrix and m-PDA curing agent, Drzal et al. (1983) have shown that both stiffness and toughness of the matrix can be changed by changing the amount of m-PDA. In this study, the matrix was cast with two different ratios of m-PDA, as mentioned in the *Materials* section. The tensile stress–strain responses of these specimens were determined by mounting strain gauges (Micro Measurement CEA-0-032UW-120) to these specimens and loading them to failure. The loading rate was 0.25 mm/min (0.01 in./min); the data were recorded on a Macintosh IIci computer; and two specimens were tested for each m-PDA ratio. The average properties of these two types of matrix materials are listed in Table 1. Representative stress–strain curves for these specimens are shown in Figure 1; the broken specimens are shown in Figure 2.

Single-fiber composite specimens with wavy fiber geometries were cast using the two different curing-agent-to-matrix ratios. A single graphite fiber was passed through the dogbone cavity of a silicone mold and the ends of the fiber were glued to aluminum tabs outside the mold (Fig. 3). To make specimens with wavy fiber geometries, the fiber in the mold was kept longer than the mold length. The matrix and curing agent mixture was mixed, debulked in a vacuum at 75°C (167°F) for about 10 minutes and then poured into the dogbone cavity of the silicone mold. The single-fiber composite was then cured with the two-step cycle in air. One of the problems that was frequently encountered in fabricating the wavy fiber specimens

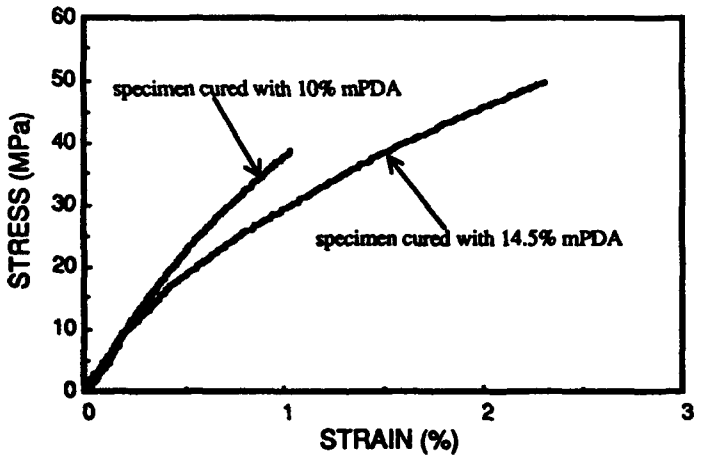

Figure 1. Effect of the hardener ratio on the stress–strain response of EPON 828–m-PDA matrix. Lowering the m-PDA ratio from its stoichiometric value (14.5 phr) results in a stiffer and more brittle matrix material.

Figure 2. Fractured specimens with strain gauges.

was that, when the matrix was poured into the cavity, the wavy fiber had a tendency to attach itself to the side walls of the mold. To stop the fiber from sticking to the walls, it was carefully pulled away from the walls by dragging it with the help of a clean pin. This process had to be repeated several times during the curing cycle until the matrix material started to gel. Once the gelation started, the wavy fiber stayed in its place. Figure 4 shows the wavy fiber geometry produced by this method in one of the specimens that was cured with 14.5% m-PDA.

In the single-fiber composite specimens cured with 10% m-PDA, an interesting phenomenon was observed in the embedded fiber. When the cured specimens were examined under polarized light, they showed another type of highly regular waviness pattern (Fig. 5). The wavelengths of these waviness patterns were much smaller. Such waviness was always present in the 10% m-PDA specimens, but it was never seen in the 14.5% m-PDA specimens. The exact mechanisms that causes such a phenomenon is currently being investigated.

The cured specimens were removed from the mold and loaded in a tensile loading fixture attached to an optical microscope. This jig allowed the real-time scanning of the specimen while it was being loaded. The loading rate was controlled by a stepper motor, which in turn was driven by a computer. As mentioned, the loading rate was 0.25 mm/min. The deformation and failure process was observed through polarized and unpolarized lights, and the images were recorded on a video cassette and on Polaroid films.

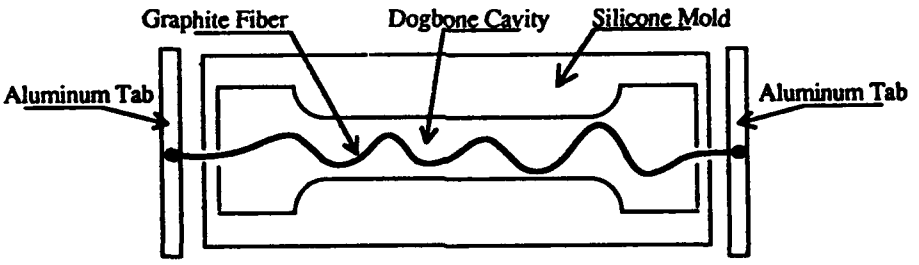

Figure 3. Arrangement used to place fiber with wavy geometry.

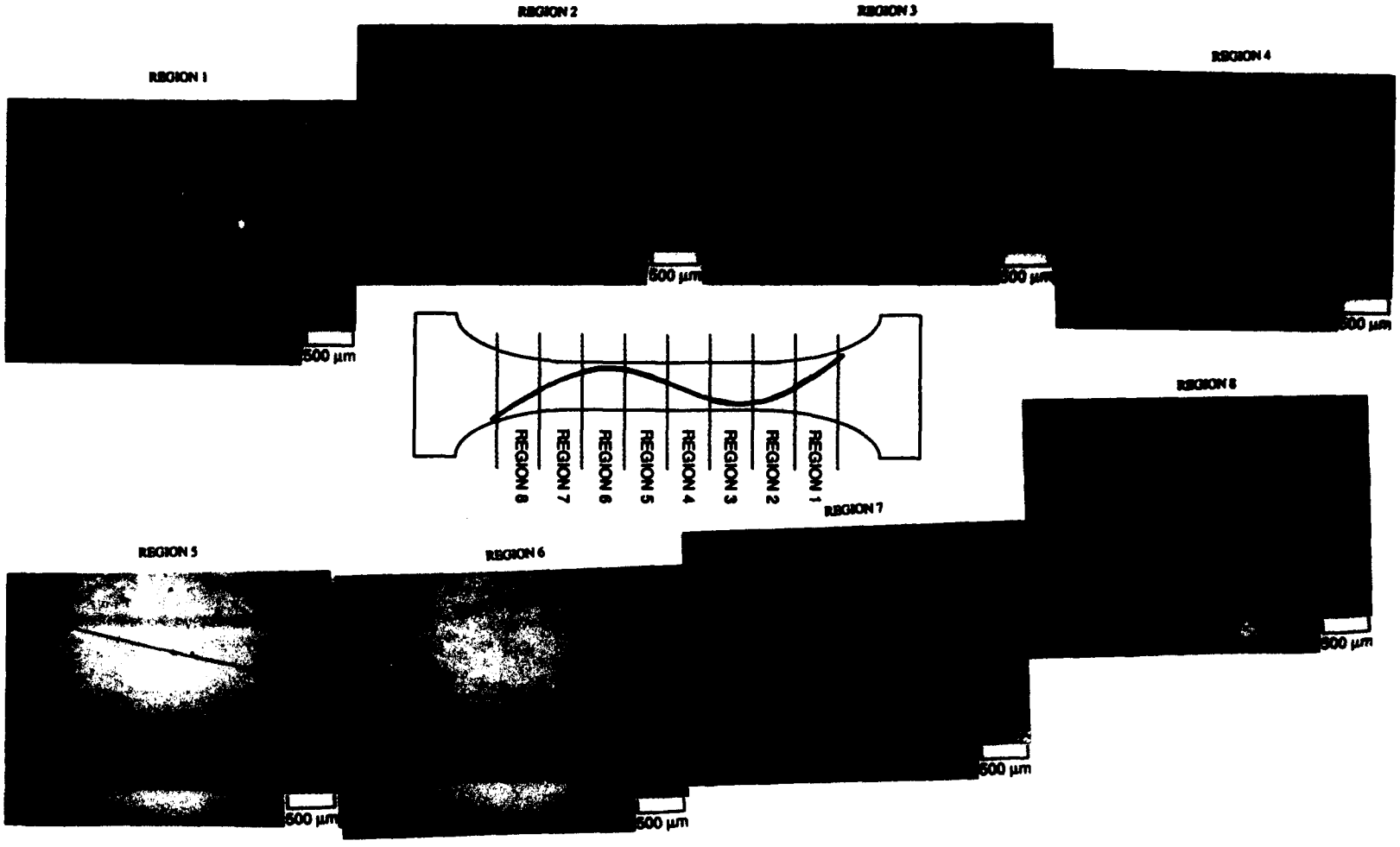

Figure 4. Wavy fiber geometry produced while laying the fiber in a single graphite fiber–epoxy specimen cured with 14.5% m-PDA.

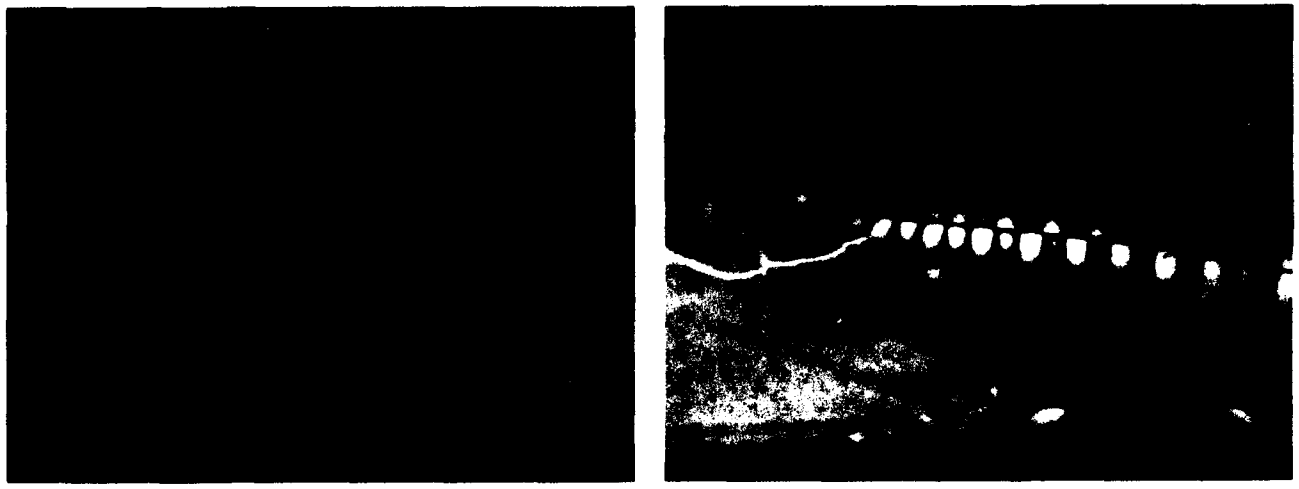

a. Magnification of 25×.

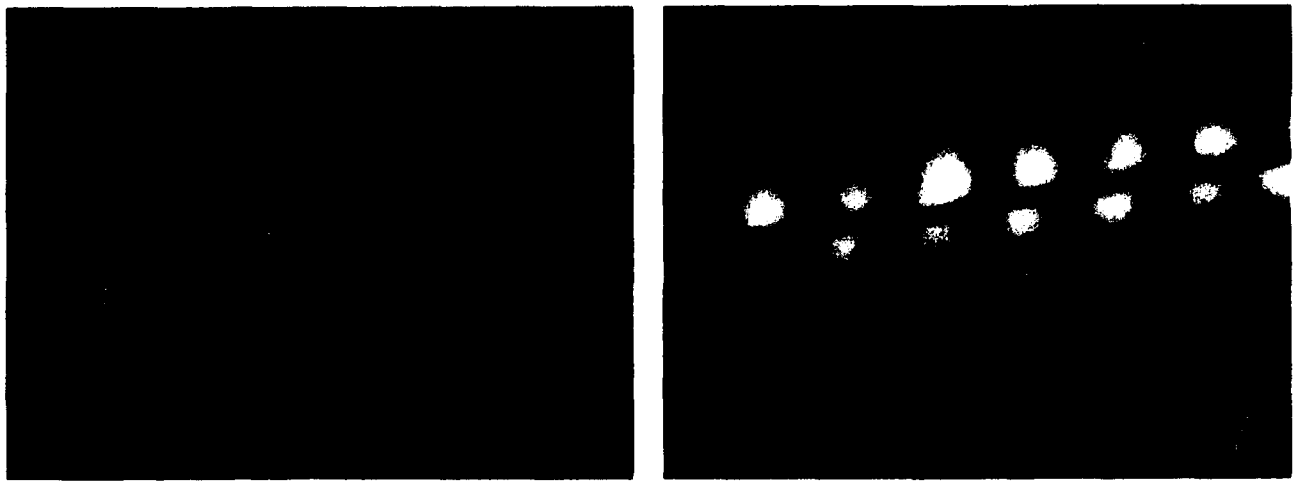

b. Magnification of 100×.

Figure 5. Fiber waviness that occurred during the curing of a single graphite fiber–epoxy specimen with 10% m-PDA.

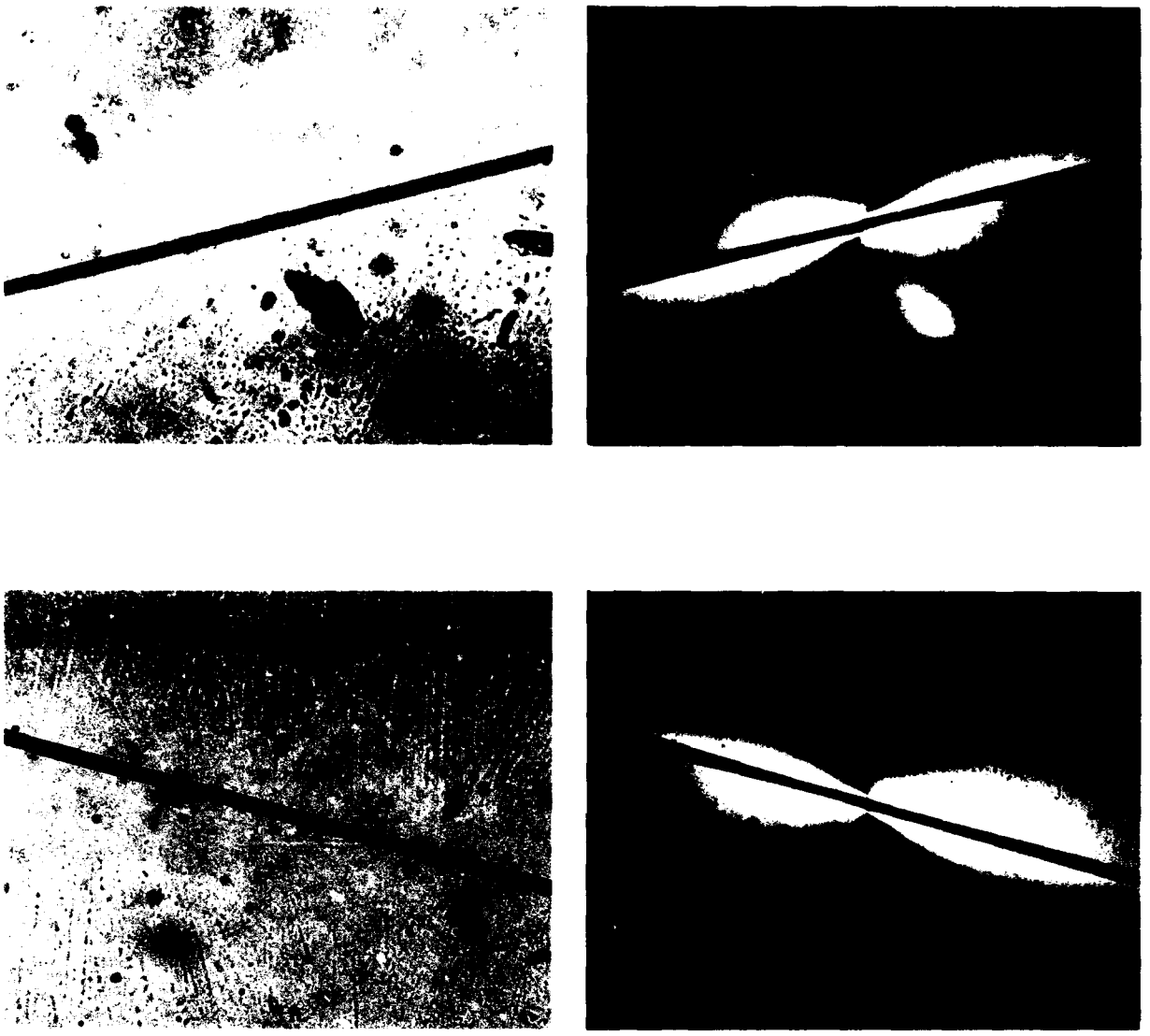

a. Transmitted light, magnification of 250×. *b. Polarized light, magnification of 250×.*

Figure 6. Fiber cracks and polarized fringe patterns seen during the tensile loading along the horizontal line of 14.5% m-PDA samples. Figure 6a shows fiber cracks that do not extend into the neighboring matrix.

RESULTS AND DISCUSSION

During the tensile loading of all the single-fiber specimens, the fiber and interfacial failure process was continuously scanned under polarized and unpolarized light to detect the location of first fiber failure. Generally, the first crack appeared at a lower applied load in the lower stiffness (14.5% m-PDA) samples. This is expected because, in the lower stiffness specimens, a given applied load produces a larger strain. Figure 6 shows polarized and unpolarized photographs of the fiber cracks observed in the 14.5% m-PDA specimens. These cracks were observed at an applied tensile stress of 35 MPa (5 Kips/in.^{2}). The polarized pictures (Fig. 6b) clearly indicate asymmetrical (with respect to the fiber axis) fringe patterns around the broken fiber ends. The fiber cracks can be seen in Figure

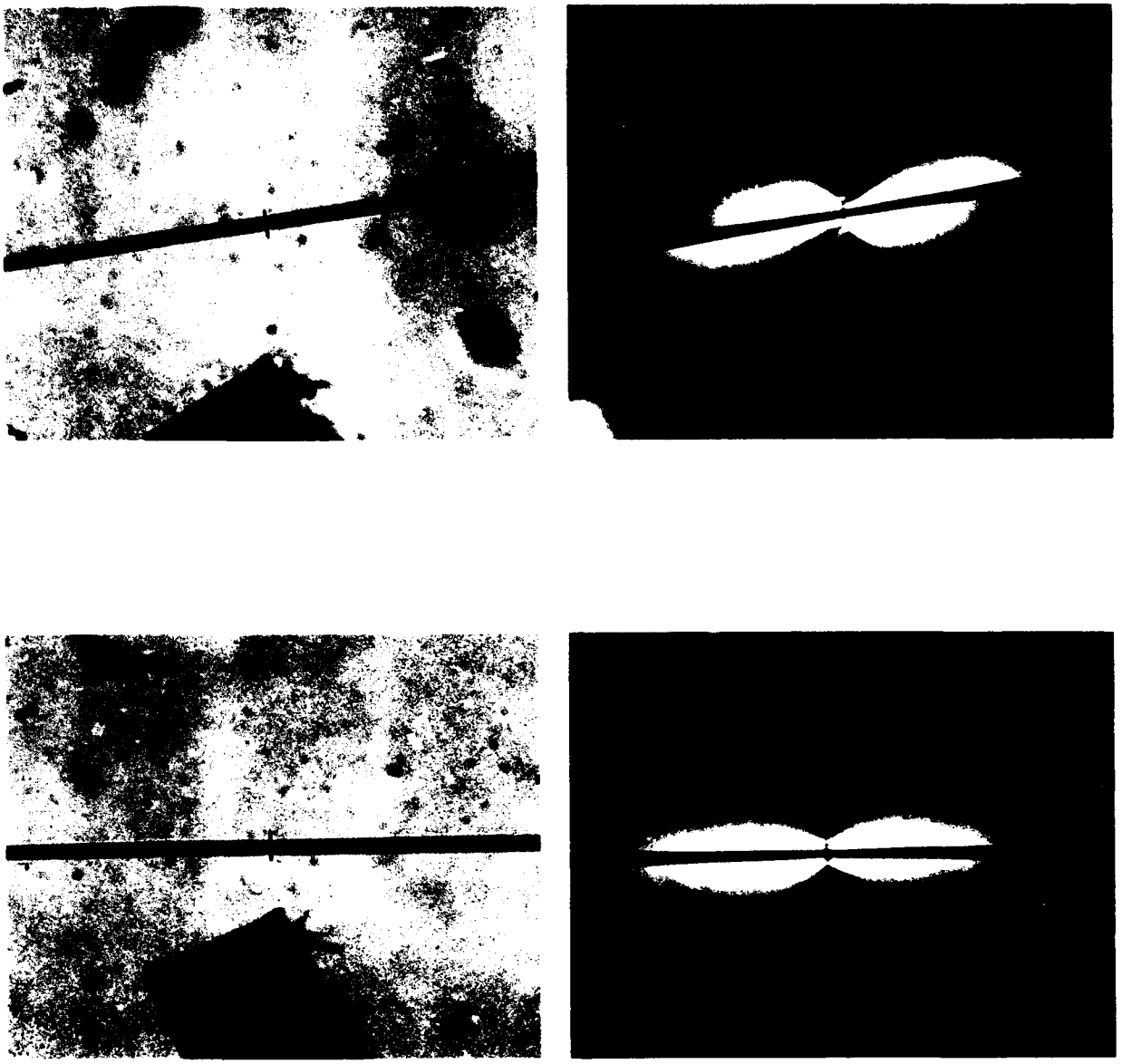

a. Transmitted light, magnification of 250×. *b. Polarized light, magnification of 250×.*

Figure 7. Fiber cracks and polarized fringe patterns seen during the tensile loading of 10% m-PDA samples. Figure 7a shows fiber cracks that extend deep into the neighboring matrix, thus producing needle-shaped matrix cracks.

6a. These cracks are perpendicular to the fiber axis and they do not extend deep into the matrix material.

Figure 7 shows fiber cracks and the fringe patterns for a 10% m-PDA specimen. These cracks were observed at an applied stress of 52 MPa (7.5 Kips/in.^{2}). Again, for the fiber cracks lying on a portion of the fiber that is at an angle to the loading axis, the polarized fringe patterns are asymmetrical at the broken fiber ends. This indicates the presence of a different stress state around the circumference of the fiber, whereas, for the crack that is lying on a portion of a fiber that is parallel to the loading axis, the fringe patterns are symmetrical. These stress patterns can be understood by examining how the interface is loaded in the

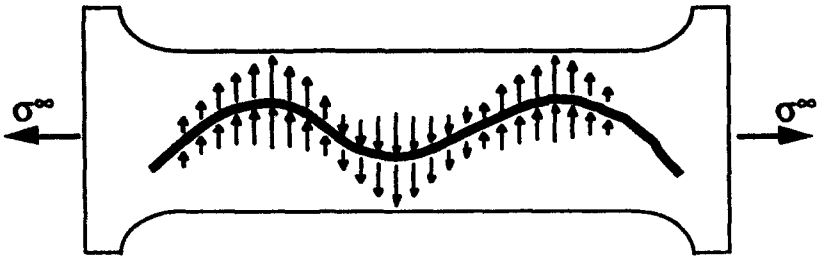

Figure 8. Interface tensile stresses around a wavy fiber.

two different cases. When the fiber is parallel to the loading axis, the interface carries only the shear stress. However, when the fiber is at an angle to the loading axis, it has a tendency to align itself parallel to the loading direction. As a result, the interface at the wavy fiber is subjected to shear stresses as well as the transverse tensile stresses on one side and the shear stresses and the transverse compressive stresses on the other side of the fiber. These transverse tensile and compressive stresses are schematically shown in Figure 8.

Another interesting observation that can be made from the results shown in Figures 6 and 7 is that, for the specimens cured with 10% m-PDA, the fiber cracks extend deep into the matrix material, thus producing characteristic long, needle-shaped matrix cracks (see Fig. 7a). In the 14.5% m-PDA specimens, the fiber cracks did not penetrate the neighboring matrix material (see Fig. 6a). The specimens cured with 10% m-PDA contain the matrix that has low fracture toughness or low strain to failure (Fig. 1). Therefore, when the fiber fractures inside the matrix, the high stress concentration at the broken fiber ends can easily cause the local fracture of the brittle matrix material and produce sharp matrix cracks. Since these cracks are perpendicular to fiber axis, they must contribute to the reduction of tensile strength of compos-

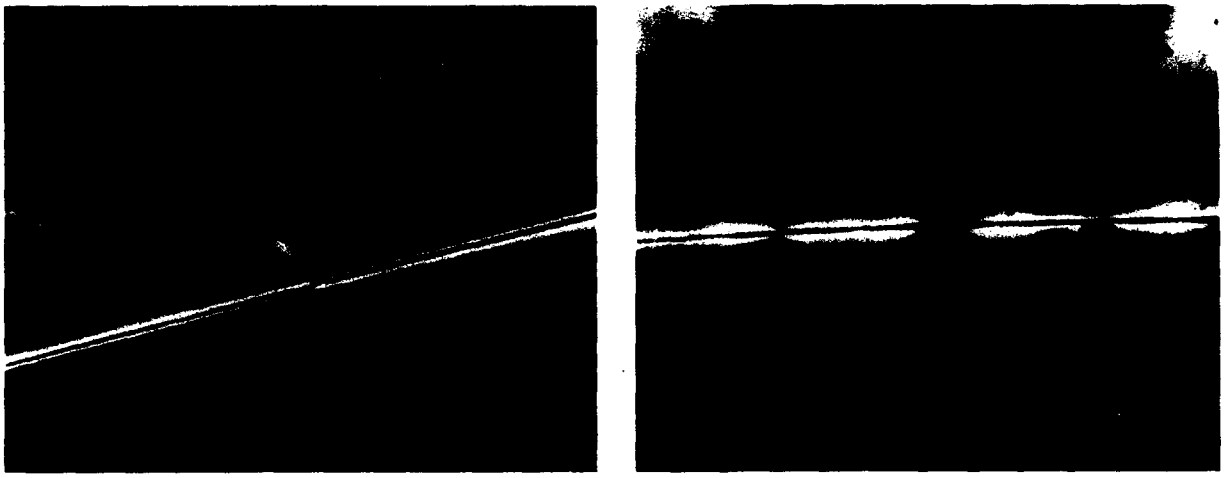

a. Fiber at an angle to loading axis.

b. Fiber parallel to loading axis.

Figure 9. Growth of polarized fringe patterns with increasing applied tensile load. Fringe patterns are much more elongated for the fiber section that is at an angle to the loading axis. More fiber fragments are observed in the fiber section that is parallel to the loading axis. The loading axis is in the horizontal direction; magnification is 100×.

ites. In the case where the matrix has large strain to failure, the high stresses at broken fiber ends may be relieved by matrix deformation or by interfacial failure, or both.

When the tensile load on the single-fiber specimens continues to increase, more and more fiber fragments are created. In addition, the fringe patterns produced at the broken fiber ends are elongated and extended in the direction away from the broken end (Fig. 9). The fringe patterns indicate high shear stresses near the broken fiber ends. The high shear stresses result when the matrix prevents the fiber from springing back after it is broken. In the portions of the fiber where it is at an angle to the loading axis, there will be both shear stress and transverse tensile stress present at the fiber surface, as shown schematically in Figure 8. The transverse tensile stresses cause the premature failure of the fiber/matrix interface. As a result, when the fiber is at an angle to the loading axis, the stresses are not efficiently transferred from the matrix to the fiber and additional fiber fragments are not produced. Instead, the fiber matrix interfacial failure propagates parallel to the fiber. This interfacial failure is indicated by the narrow and much elongated fringe patterns along the fiber length in Figure 9a.

Also seen in Figure 9a is a long gap between the broken fiber ends. For the regions where fiber is parallel to the loading axis, such long gaps between broken fiber ends were not observed. A possible reason for such a behavior is that the extensive interfacial debonding near the fiber lying at an angle to the loading axis makes the fiber lie loosely in the matrix tunnel (the evidence of a matrix tunnel is further given below). As a result the fiber can spring back freely after its failure. In the regions where fiber is parallel to the loading axis, the fringe patterns are much wider, suggesting much less extensive interfacial debonding. More fiber fragments are produced in these regions as the applied load is increased. In such situations the matrix surrounding the fiber prevents the fiber from springing back after its failure. This suggests that the waviness keeps the fibers from being loaded to their full capacity, thus resulting in the poor tensile properties. Generally, in the failed single-fiber specimens, there were more fiber fragments in the 14.5% m-PDA specimens than in the 10% m-PDA specimens. Such a difference can be attributed to the high stiffness and low failure strain of 10% m-PDA specimen. These specimens may have failed before the saturation of the fiber fragmentation process.

The applied tensile load on the single-fiber specimens was increased until fracture. Examination of the failed ends of the specimen under an optical microscope revealed a significant fiber pull-out in several specimens. An example of one such fiber pull-out in a 14.5% m-PDA specimen is shown in Figure 10. Figure 10a shows the matrix tunnel produced by the pulled out graphite fiber; Figure 10c is the polarized photo of Figure 10a. A comparison among Figures 10a, b and c clearly shows that when a fiber breaks during tensile loading, there is a significant fiber–matrix debonding on either side of the broken fiber ends, i.e., the fiber is loosely held in the matrix tunnel. This suggests that the elongated fringe patterns seen in Figure 9a represent extensive fiber–matrix debonding near the broken fiber ends. Figure 11 shows the matrix tunnel produced by fiber pull-out in the 10% m-PDA specimen. In this specimen, where the matrix material is relatively more brittle, pieces of matrix material have also been pulled out of the broken specimen. These matrix pieces are seen emanating from the needle-shaped matrix cracks Figure 11b.

CONCLUSIONS

Experiments were conducted on specimens made of a single wavy graphite fiber in an epoxy matrix, where the matrix's properties were changed by changing its ratio with m-PDA curing agent. Two ratios—10 and 14.5%—were selected. The matrix with lower m-PDA ratio was stiffer and more brittle. On the basis of observations via an optical microscope of the fiber and interface failure process during the tensile loading of these composites, the following conclusions have been made:

1. Both lower and higher stiffness samples produced fiber fragmentation during the tensile loading.

2. The tensile loading of samples with the more stiff and brittle matrix produced fewer fiber fragments. However, because of the presence of a wavy fiber, the fragment length varied significantly along the specimen length within the same specimen.

3. During the tensile loading of samples containing the low-toughness matrix, long, needle-shaped matrix cracks emanated from the fiber broken ends. Such cracks were not observed in samples in which the matrix failure strain was larger. Since the matrix toughness decreases at

a. Matrix tunnel.

b. Pulled-out fiber.

c. Polarized light.

Figure 10. Fiber pull-out and the corresponding matrix tunnel formed during the fracture of a 14.5% m-PDA sample (magnification of 250x).

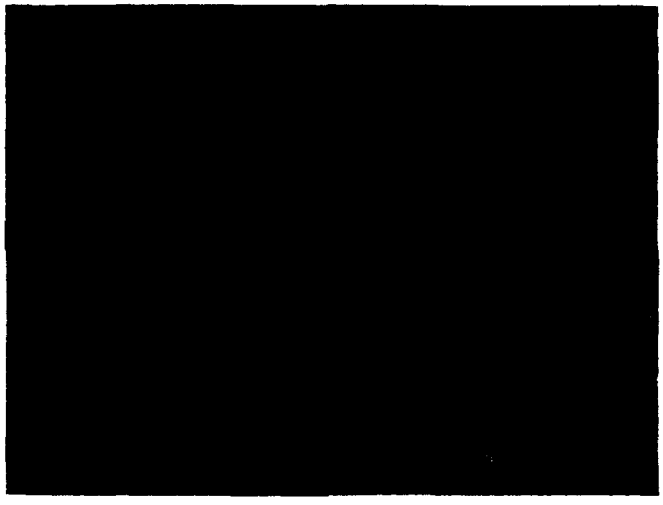

a. Transmitted light, magnification of 250×.

b. Polarized light, magnification of 250×.

Figure 11. Matrix tunnel formed during the fracture of a 10% m-PDA sample.

low temperatures, these long matrix cracks in the low-toughness matrix composites are believed to be responsible for the reduction of tensile strength at low temperatures.

4. There was significant interfacial failure near broken fiber ends in regions where the fiber was at an angle to the loading axis. The interfacial failure was much less extensive in areas where the fiber was parallel to the loading axis. In these regions, the embedded fiber broke into smaller fragments. The presence of transverse tensile stresses at the interface in the former case is believed to be responsible for the extensive fiber/matrix interfacial failure.

5. The fractured specimens showed fiber pullout and the corresponding matrix tunnel. This suggests that, during the tensile loading, there is extensive fiber–matrix debonding at the broken fiber ends.

LITERATURE CITED

Bader, M.G. (1988) Tensile strength of uniaxial composites. *Science and Engineering of Composite Materials*, **1:** 1–11.

Drzal, L.T., M.J. Rich, M.F. Koenig and P.F. Lloyd (1983) Adhesion of graphite fibers to epoxy matrices: II. The effect of fiber finish. *Journal of Adhesion*, **16:** 133.

Dutta, P.K. (1992) Tensile strength of unidirectional fiber composites at low temperatures. *Japan–US Conference on Composite Materials, June 22–24, 1992*, pp. 782–792.

Madhukar, M.S. and L.T. Drzal (1991) Fiber-matrix adhesion and its effect on composite mechanical properties: II. Longitudinal (0°) and transverse (90°) tensile and flexure behavior of graphite/epoxy composites. *Journal of Composite Materials*, **25:** 958–991.

REPORT DOCUMENTATION PAGE

Form Approved
OMB No. 0704-0188

1. AGENCY USE ONLY (Leave blank)	2. REPORT DATE	3. REPORT TYPE AND DATES COVERED
	April 1994	

4. TITLE AND SUBTITLE
Effect of Matrix Stiffness on Wavy Fiber Behavior in Single-Carbon-Fiber–Epoxy Composites

5. FUNDING NUMBERS
PR: 4A762784AT42
TA: SS
WU: 019

6. AUTHORS
Madhu S. Madhukar and Piyush K. Dutta

7. PERFORMING ORGANIZATION NAME(S) AND ADDRESS(ES)
U.S. Army Cold Regions Research and Engineering Laboratory
72 Lyme Road
Hanover, N.H. 03755-1290

8. PERFORMING ORGANIZATION REPORT NUMBER
Special Report 94-10

9. SPONSORING/MONITORING AGENCY NAME(S) AND ADDRESS(ES)
Office of the Chief of Engineers
Washington, D.C. 20314-1000

10. SPONSORING/MONITORING AGENCY REPORT NUMBER

11. SUPPLEMENTARY NOTES

12a. DISTRIBUTION/AVAILABILITY STATEMENT
Approved for public release; distribution is unlimited.
Available from NTIS, Springfield, Virginia 22161

12b. DISTRIBUTION CODE

13. ABSTRACT (*Maximum 200 words*)

This research identifies the mechanisms responsible for lowering the tensile strength of unidirectional polymer matrix composites at low temperatures. Since the stiffness of polymer matrices increases and toughness decreases when the temperature is lowered, the effect of low temperature was simulated by changing the matrix stiffness and toughness. Composite specimens containing a single carbon fiber embedded in an epoxy matrix were cast. The fibers were cast in curved geometries, and the specimens were loaded in tension. The fiber and interfacial failure processes were observed under polarized and unpolarized light through an optical microscope. Increasing the tensile load on the single fiber–epoxy specimens broke the embedded fiber into small fragments, whose lengths were smaller in the regions where the fiber was lying parallel to the loading axis. A significant fiber/matrix interfacial debonding, observed near the broken fiber ends in all specimens, was much more pronounced when the fiber was at an angle to the loading axis. Transverse tensile stresses at the interface caused this interfacial debonding. Specimens with higher matrix stiffness had long matrix cracks at the broken fiber ends, which were perpendicular to the fiber axis. These matrix cracks tend to propagate perpendicular to the fiber axis, increasing the composite's cold sensitivity. The major conclusions are as follows: 1) When fibers are wavy, they are not loaded to their full capacity because of premature interfacial debonding started by the interfacial shear stresses and the transverse tensile stresses. The transverse tensile stresses at the interface are not present in the straight fiber specimens. 2) At higher stiffness and lower toughness values, the matrix cracks emanating at the broken fiber ends make the composite weaker. These two sources lower the strength of unidirectional composites at low temperatures.

14. SUBJECT TERMS
Composites; Interfacial bond; Polymer composites; Composite tensile strength; Matrix crack; Wavy fiber

15. NUMBER OF PAGES
18

16. PRICE CODE

17. SECURITY CLASSIFICATION OF REPORT	18. SECURITY CLASSIFICATION OF THIS PAGE	19. SECURITY CLASSIFICATION OF ABSTRACT	20. LIMITATION OF ABSTRACT
UNCLASSIFIED	UNCLASSIFIED	UNCLASSIFIED	UL